

Frequency Domain Image Translation: More Photo-realistic, Better Identity-preserving

Mu Cai¹ Hong Zhang² Huijuan Huang² Qichuan Geng³ Gao Huang⁴

¹University of Wisconsin-Madison ²Kwai Inc. ³Beihang University ⁴Tsinghua University

mucai@cs.wisc.edu fykalviny@gmail.com huanghuijuan@kuaishou.com
zhaokefirst@buaa.edu.cn gaohuang@tsinghua.edu.cn

Abstract

Image-to-image translation aims at translating a particular style of an image to another. The synthesized images can be more photo-realistic and identity-preserving by decomposing the image into content and style in a disentangled manner. While existing models focus on designing specialized network architecture to separate the two components, this paper investigates how to explicitly constrain the content and style statistics of images. We achieve this goal by transforming the input image into high frequency and low frequency information, which correspond to the content and style, respectively. We regulate the frequency distribution from two aspects: a) a spatial level restriction to locally restrict the frequency distribution of images; b) a spectral level regulation to enhance the global consistency among images. On multiple datasets we show that the proposed approach consistently leads to significant improvements on top of various state-of-the-art image translation models.

1. Introduction

Image-to-image translation aims at translating a particular style of an image into another. The images are visually distinctive and each image corresponds to a unique style. For example, when changing the decoration style of churches, the style would refer to the color or illumination. This task has been significantly improved as the introduction of Generative Adversarial Network (GAN) [16, 34]. However, such methods focus on extracting the average style difference between two sets of images, which lack the ability of capturing diverse styles in the dataset.

Recent works [5, 14, 6, 24] have shown that the synthesized images can be more photo-realistic if decomposing the images into the *content*, and *style*, and enforcing the combination of these two independent components. Here, the content refers to the identifying characteristics of images, such as the sketch, pose and sharp edges, and the

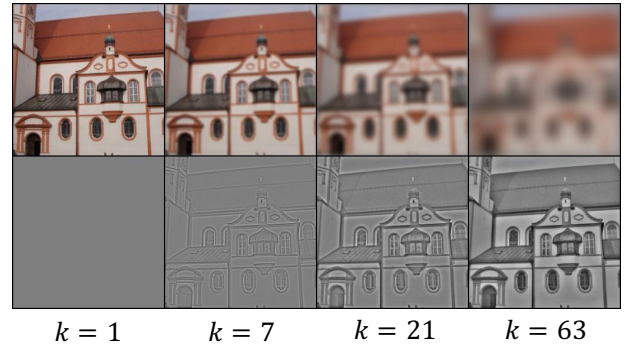


Figure 1: Visualization of the effect of decomposing the original image using Gaussian blurring with different kernel sizes. The first row denotes the low frequency images after blurring, and the second row represents the corresponding grayscale scale high frequency images.

style denotes as the global texture statistics like color distribution, illumination and even the weather. To disentangle the two components, the style is always compressed to low resolution features to remove the spatially redundant information; while the content is represented by relatively high resolution features to encourage the spatial structure to be similar to the given image. Unfortunately, such methods mainly focus on designing specialized network architectures. In comparison, less effort has been made to explicitly constrain the content and style statistics of images.

In this paper, we propose the *Frequency Domain Image Translation* (FDIT) to explicitly optimize the preservation of the content and style information, which can significantly improve the performance of the state-of-the-art image translation models. Our method is motivated by an intriguing observation in frequency analysis. When mapping the raw image into the frequency space according to the varying speed of pixels around their spatial locations, we could obtain an optimal disentangled representation of the content and style. To illustrate this point, Fig. 1 shows the resulting images via adopting the *Gaussian blur* to decompose the original

image into different spatial frequencies. The upper images correspond to the smoothly varying components like color and illumination; while the lower images depict the content of the original image which is consistent with the rapidly changing features in the pixel space, such as sharp edges and the overall pose. The spatial information contained by these two types of the images tends to grow in the opposite direction as the kernel size increasing. Therefore, when choosing a suitable kernel, the resulting images should ideally correspond to decoupled features of the content and the style.

Specifically, given an original image and its associated reconstruction image, we transform them into high frequency images and low frequency images respectively, and encourage such outcomes to be similar. In this way, we can regulate the frequency distribution of images while maintaining the associated spatial information. Nevertheless, such spatial level supervision remains in a local manner due to the fact that the convolution is only operated within the neighborhood of pixels, which would inevitably ignores the global statistics in frequency space. In order to restrict the global distribution of the frequency features, we directly apply Fast Fourier Transform (FFT) to get the power spectrum and impose the reconstruction upon it. Thus, each spatial frequency component in FFT would represent the information from all pixels across the image. Similarly, these ideas are adopted for the regulation of the synthesized image, which is desired to maintain the content of the original image. Therefore, we explicitly constrain the distribution of their frequency information in both the spatial and spectral level. Furthermore, two frequency domain assisted modules named Adaptive Frequency Feature Embedding module and Frequency-assisted Patch Discrimination module are designed to encourage the network to learn the instance-wise frequency information better.

Although being simple, the proposed FDIT is highly effective and complements existing image-to-image translation methods. Extensive experiments on multiple datasets demonstrate that the proposed method consistently improves the performance of state-of-the-art image translation models.

2. Related work

Generative adversarial network (GAN) [9] is known for its powerful ability in generating realistic images. GAN has revolutionized many computer vision tasks, such as super resolution [22, 29], colorization [15, 32], and image synthesis [3, 23, 7]. Early work [25, 13] directly used the Gaussian noises as the seeds to generate images via the supervision of the discriminator. However, this approach is shown to be weak in generating photo-realistic images. Recently, borrowing the adaptive instance normalization (AdaIN) module [12] from image stylization, a series of

works boosted the image reality into a new level by injecting the noises hierarchically [19, 20] in the generator.

Image-to-image translation. The above models only accept noises as the input of the generator, making the generated images also randomly distributed. However, in real-world applications, the goal is to process *real images*, instead of producing random images. Under this context of the image-to-image translation task, we would like the generated image to follow the style of the reference image while keeping the content of the source image. One way to achieve this is to use the GAN inversion method to map the real image space back into the noises space via the optimization method [1, 2, 20]. However, these methods are known to be quite time-consuming due to its slow iterative optimization process. Furthermore, the quality of the reconstructed images is unsatisfactory, which makes such methods hard to be deployed in mobile devices. Another way to achieve this goal is to utilize the conditional GAN (autoencoder) to convert the input images into latent vectors [14, 5, 6, 24], which could produce images in a feed forward way, making the image translation process much faster than the former one. However, such model architectures are not a reliable guarantee of effective decoupling, observed by the generated images in the most of the state-of-the-art deep image translation model such as StarGAN v2 [6] and Swapping Autoencoder [24].

Frequency domain in deep learning. Frequency domain is known to be powerful in analyzing images in traditional image processing. The key idea of frequency analysis is to map the pixels from the Euclidean space to frequency space according to the changing speed in spatial domain. Several works tried to bridge the connection between deep learning and frequency analysis. Chen *et al.* [4] and Xu *et al.* [30] argued that by incorporating frequency transformation, the neural network could be more efficient and effective. Another work [28] found that the high frequency components are helpful to explain the generalization of neural networks. Later, Durall *et al.* [8] observed that the images generated by GAN are heavily distorted in high-frequency parts, and they introduced a spectral regularization term to the loss function to alleviate this problem. However, no prior works tried to analyze the problems of the images to image translation task under the frequency domain. In this work, we are the first to explicitly optimize the *image translation* task by regularizing the frequency information.

3. Frequency Domain Image Translation

In this section, we first set up the model in the image-to-image translation task. Then we discuss our proposed frequency based identity-preserving framework in detail. Roughly, a *spatial level* restriction is introduced to locally preserve the frequency distribution. Then a *spectral level* regulation is proposed to further enhance the distribution

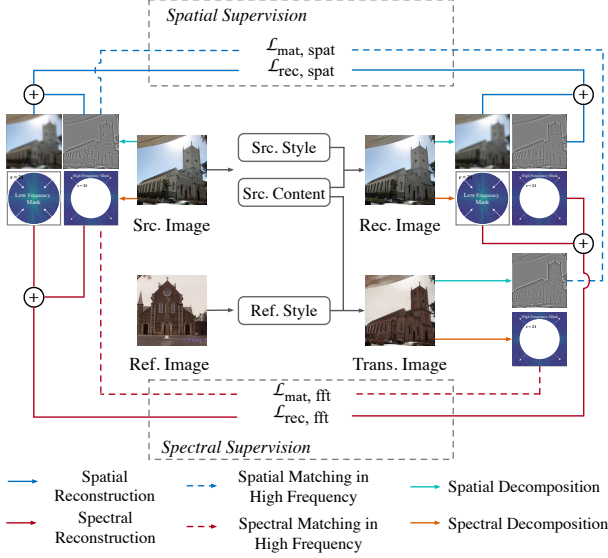


Figure 2: The illustration of the proposed frequency based image translation framework FDIT.

from the global perspective. Fig. 2 gives an overview of the proposed approach.

3.1. Image-to-image Translation

Image-to-image translation aims at directly generating the synthesized image given a source image. Under the scenarios of real-word applications, there is usually an accompanying reference image guiding the resulting style during the translation process.

In the general deep image translation framework, an image embedding module is always employed in addition to the general GAN structure, serving as the feature extractor for the content and style. To be specific, given an image $\mathbf{x} \sim \mathbf{X} \subset \mathbb{R}^{H \times W \times 3}$, the embedding module E and generator G form a mapping of the latent code $\mathbf{z} \sim \mathbf{Z}$ between two images. Here the latent space \mathbf{Z} is usually composed of two components, $\mathbf{z} = (\mathbf{z}_c, \mathbf{z}_s)$, which is desired to represent the content and style information in a decoupled way. However, such former models make less effort to incorporate explicit restrictions for the decoupled encoding.

For this kind of image embedding based models, they only impose pixel-level reconstruction in image space, which is insufficient with respect to the identity-preserving image translation tasks. Motivated by the frequency analysis theory in image processing, we find that high frequency components match the content features quite well, such as the sharp edges; while the low frequency components have a close relationship with the style information, like the color and illumination. Therefore, we introduce novel objectives and network modules to explicitly impose restrictions on the frequency domain which could pose a stronger guarantee of the content and style decoupling.

3.2. Frequency based Training Objectives

Preserving the frequency distribution in the spatial level.

In order to transform the pixel-level features into frequency-level features while preserving the spatial information, we utilize a fuzzy filter, *e.g.*, Gaussian kernel, to filter the high frequency component and leave the low frequency information. The Gaussian kernel k can be defined as:

$$k_\sigma[i, j] = \frac{1}{2\pi\sigma^2} e^{-\frac{1}{2} \left(\frac{i^2 + j^2}{\sigma^2} \right)}, \quad (1)$$

where $[i, j]$ indexes the position in the image, and σ^2 denotes the variance of the Gaussian function, which grows proportionally with the Gaussian kernel size.

Thus, the low frequency information can be represented as the *blurred* image \mathbf{x}_L using convolution of this kernel.

$$\mathbf{x}_L[i, j] = \sum_m \sum_n k[m, n] \cdot \mathbf{x}[i + m, j + n]. \quad (2)$$

An intuitive way to obtain the high frequency image is to subtract the low frequency information \mathbf{x}_L from the raw image \mathbf{x} . Nevertheless, the high frequency image is far from optimal due to the existing of the color or illumination information. To address this issue, we first transform the resulting color image into the grayscale image, and then high frequency information would be extracted by:

$$\mathbf{x}_H = \text{r2g}(\mathbf{x}) - (\text{r2g}(\mathbf{x}))_L, \quad (3)$$

where r2g is short for the `rgb2gray` function, converting the color image to the grayscale image. In this way, the color and illumination in the low frequency image \mathbf{x}_L are preserved while the fine details are wiped out. Meanwhile, with the help of the `rgb2gray` function, the high frequency image \mathbf{x}_H almost contains the sharp edges, *i.e.* *sketch* of the original image.

Considering the reconstruction quality in the frequency domain, the overall loss over the blurred image and the high frequency grayscale image can be formulated as:

$$\mathcal{L}_{\text{rec,spat}}(E, G) = \mathbb{E}_{\mathbf{x} \sim \mathbf{X}} [\|\mathbf{x}_L - (G(E(\mathbf{x})))_L\|_1 + \|\mathbf{x}_H - (G(E(\mathbf{x})))_H\|_1]. \quad (4)$$

Moreover, under the image translation models, we would like the resulting images adhere to the content of the original image. Therefore, regulating the high frequency components would ideally meet what we want to match during training. Hence, we enforce that the generated image should share the same high frequency images with the original content image. The high frequency match loss $\mathcal{L}_{\text{mat,spat}}$ can be formalized as:

$$\mathcal{L}_{\text{mat,spat}}(E, G) = \mathbb{E}_{\mathbf{x} \sim \mathbf{X}} [\|\mathbf{x}_H^1 - (G(\mathbf{z}_c^1, \mathbf{z}_s^2))_H\|_1], \quad (5)$$

where \mathbf{z}_c^1 and \mathbf{z}_s^2 are the content code of the source image and the style code of the reference image, respectively.

Preserving the frequency distribution in the spectral level. In the previous paragraph, we introduced how to represent high/low frequency information in the spatial level. However, due to the fact that each pixel's value in \mathbf{x}_L and \mathbf{x}_H is only affected by the pixels within the convolution kernel, the frequency features of images are limited in a local manner. Here we introduce a method to help the disentanglement of content and style from the global perspective. One ideal way to enhance the frequency information is to use Fast Fourier Transform (FFT) to directly map the \mathbf{x} from image space to the spectral space. Each point in the spectrum would utilize information from all pixels according to the discrete spatial frequency, which would represent the frequency features in the global level. Furthermore, the pixels' spatial information would be fully wiped out while frequency information would be maintained, which is a favorable restriction in our context.

Actually, the frequency features obtained by the Gaussian kernel and FFT contain the same underlying information, and the only difference lies in the representation form. As shown in Fig. 3, if we transform the images in Fig. 1 into the spectrum space, then the FFT response of high/low frequency images ideally fits in with the source image in two respective regions. The effects of the Gaussian kernel size are also clearly reflected in the image. To be specific, a large kernel would cause serious distortion on low frequency band while a small kernel would drop much of the high frequency information. In this work, we choose the kernel size $k = 21$, which could appropriately separate the high/low frequency information, demonstrated in both image space and spectral space distribution.

Therefore, on top of the aforementioned loss function in Sec. 3.2, we further propose to use Fast Fourier Transform (FFT) to restrict the frequency feature distribution from the global perspective. To be specific, we apply Discrete Fourier Transform \mathcal{F} on a real sequence 2D image data I of size $M \times N$:

$$\mathcal{F}(I)(k, \ell) = \frac{1}{MN} \sum_{m=0}^{M-1} \sum_{n=0}^{N-1} e^{-2\pi i \cdot \frac{mk}{M}} e^{-2\pi i \cdot \frac{n\ell}{N}} \cdot I(m, n), \quad (6)$$

for $k = 0, \dots, M-1, \ell = 0, \dots, N-1$.

We transform \mathcal{F} from the complex number domain to the real number domain for the convenience of post processing. Besides, we take the logarithm for the results to compress the range for stable training:

$$\mathcal{F}^R(I)(k, \ell) = \log(1 + \sqrt{[\text{Re}\mathcal{F}(I)(k, \ell)]^2} + \sqrt{[\text{Im}\mathcal{F}(I)(k, \ell)]^2 + \epsilon}), \quad (7)$$

where $\epsilon = 1 \times 10^{-8}$, which is a term for the numerical stability; Re and Im denote the real part and the imaginary part of $\mathcal{F}(I)(k, \ell)$ respectively.

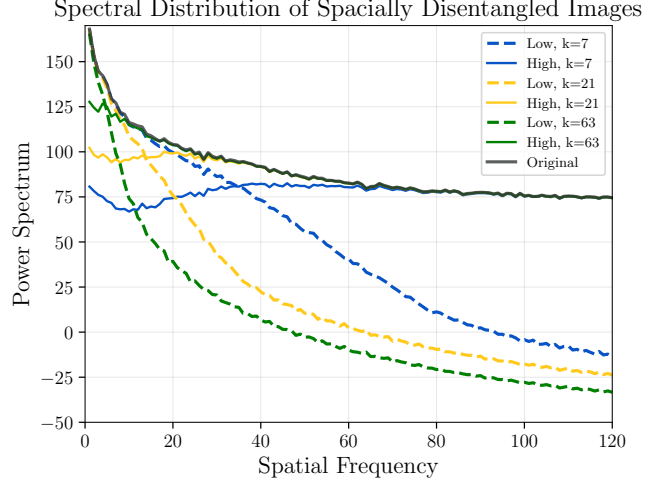


Figure 3: Transforming the resulting images in Fig. 1 into the frequency power spectrum, different frequency images ideally fit in with the original image in their respective regions.

Similar to the idea in Eqn. 4, we also regulate the reconstruction loss in the frequency spectrum:

$$\mathcal{L}_{\text{rec,fft}}(E, G) = \mathbb{E}_{\mathbf{x} \sim \mathbf{X}} [\|\mathcal{F}^R(\mathbf{x}) - \mathcal{F}^R(G(E(\mathbf{x})))\|_1]. \quad (8)$$

Here we also constrain the high frequency components of the generated images for better identity-preserving capability. According to the statistical distribution of \mathcal{F}^R across the whole training dataset, we can choose a threshold *circle* as a boundary between these two components, *i.e.*, we can get the high frequency mask M_H and low frequency mask M_L , shown in Fig. 2.

Equipped with the $\mathbf{r2g}$ transformation, the high frequency information is obtained by $\mathcal{F}_H^R(\mathbf{x}) = \mathcal{F}^R(\mathbf{r2g}(\mathbf{x})) \cdot M_H$. Following the same way, the high frequency matching loss on the spectrum can be formalized as:

$$\mathcal{L}_{\text{mat,fft}}(E, G) = \mathbb{E}_{\mathbf{x} \sim \mathbf{X}} [\|\mathcal{F}_H^R(\mathbf{x}^1) - \mathcal{F}_H^R(G(\mathbf{z}_c^1, \mathbf{z}_s^2))\|_1]. \quad (9)$$

Overall loss. Considering all the aforementioned losses, the overall loss is formalized as:

$$\mathcal{L}_{\text{freq}} = \mathcal{L}_{\text{org}} + \alpha_1 \mathcal{L}_{\text{rec,spat}} + \alpha_2 \mathcal{L}_{\text{mat,spat}} + \alpha_3 \mathcal{L}_{\text{rec,fft}} + \alpha_4 \mathcal{L}_{\text{mat,fft}}, \quad (10)$$

where \mathcal{L}_{org} is the original loss function of *any* image translation model. In this paper, we choose $\alpha_1 = \alpha_2 = \alpha_3 = \alpha_4 = 1$.

3.3. Frequency Domain Assisted Modules

Our model can be applied to any deep image translation based model, which usually consists of an image embedding module E and the vanilla GAN modules including the

generator G and discriminator D . In order to further boost the identity-preserving capability of FDIT, we introduce a novel frequency-based adaptive image translation module and a frequency-assisted patch discrimination module to the image translation models.

Adaptive frequency feature embedding module. Common image embedding modules are usually build with a stack of ResBlocks [10] or StyleBlocks [20]. However, natural images have various of contents, color, illumination, *etc.* Therefore, simple feature extractors could not reflect the characteristics of images adaptively, especially for the frequency information. Specifically, the location of high/low frequency features and the ratio between them could be quite different from image to image. Thus we propose a novel frequency feature embedding module in order to selectively highlight the channel-wise frequency components in an instance level.

To be specific, within the image embedding module, we first map the intermediate feature maps $F \in \mathbb{R}^{H \times W \times C}$ into a channel-wise attention vector $A_1 \in \mathbb{R}^{1 \times 1 \times C}$. In order to enable the network to learn the instance-wise frequency information better, we map A_1 into $A_2 \in \mathbb{R}^{1 \times 1 \times 2C}$, which is the concatenation of high/low frequency attention maps. As shown in Appendix 7.1, via incorporating the attention-based channel selection module, the network has the capability to encourage the learning of the instance-level diverse frequency distribution in a decent way.

Frequency-assisted patch discrimination module. To enhance the consistency between the styles of the reference image and the synthesized image, a large portion of deep image translation models used an additional patch discriminator [17, 24] to supervise this process. However, such module only accepts the raw pixel-level patches as the inputs, which would inevitably introduce the content information into the patch discriminator, conflicting with the role of the this module. In order to better assist the style extraction from the reference image, we obscure it using a Gaussian kernel before feeding it into the patch-wise discriminator, preventing the content information of the reference image from being ‘memorized’ by the discriminator.

4. Experiments

In this section, we evaluate our proposed method on two state-of-art image translation models, *i.e.*, Swapping Autoencoder [24], StarGAN v2 [6], and one GAN inversion model, *i.e.*, Image2StyleGAN [1]. Extensive experimental results show that our model can not only enhance the identity-preserving capability of vanilla models, but also make the generated images more photo-realistic. Even on the challenging attribute editing task, our framework could produce high-quality images that could strictly adhere to the

content of the source image. All the experiments are conducted in a validation set separate from the training process.

4.1. Autoencoder

Autoencoder is widely used as the backbone of the deep image translation task [1, 14]. We choose Swapping Autoencoder [24] to conduct the experiments, which is built on the backbone of StyleGAN2 [20]. This model also uses the technique in PatchGAN [17] to further improve the texture transferring performance.

We incorporate all the proposed frequency based components into the vanilla Swapping Autoencoder, and conduct the experiments on five datasets: (1) LSUN Church [33], (2) CelebA-HQ [18], (2) LSUN Bedroom [33], (4) Flickr Mountains (100k self-collected images), (5) Flickr Waterfalls (100k self-collected images). All the images are trained and tested at 256×256 resolution.

4.1.1 Reference-guided Image Synthesis

Firstly, we encode the content and style of the two input images, and then swap their respective components. Results show that our model could generate high-quality swapped images on diverse datasets, which could preserve the content of the source image while transferring the style from the reference image.

Identity-preserving image hybrids. The vanilla Swapping Autoencoder is poor in maintaining the outline and the local sharp edges in the source image. As shown in Fig. 4 and Fig. 5, these attributes are heavily destroyed, either distorted or blurred. Besides, the overall pose of the generated images also has a large shift from the original source image.

Fortunately, after optimizing the vanilla Swapping Autoencoder [24] with FDIT, the quality of the swapped hybrid images is highly boosted. As shown in Fig. 4 and Fig. 5, the artifacts almost disappear, and more importantly, the overall sketches and local fine details are well preserved while the coloring, illumination and even the weather are perfectly transferred from the reference image.

Here we also compare our framework with a state-of-the-art image stylization method [31]. Image stylization [31, 21] is another approach to synthesize hybrid images. However, this approach emphasizes on the strict adherence to the source image, leading to the unsatisfactory results in cross-domain image generation tasks. For example, when synthesizing images under the human face dataset, the stylization based methods can only shift the color distribution, unable to transfer the gender, shown in Fig. 5. In contrast, FDIT can generate cross-domain yet high-quality images, further demonstrating the superiority of our method in image synthesis.

Photorealistic generated images. Our model can substantially and universally improve the image quality while

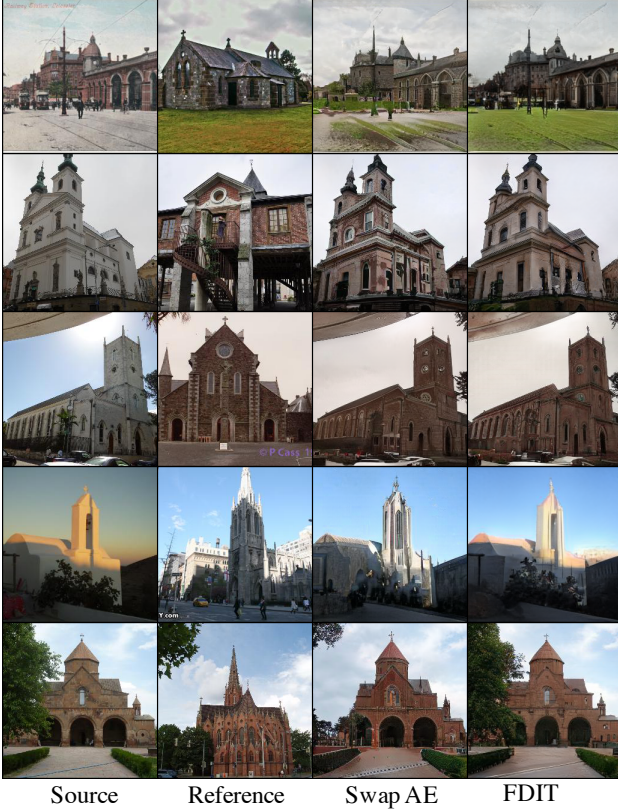


Figure 4: Image translation results of the LSUN church dataset. Four columns denote the source images, reference images, and the generated images of Swapping Autoencoder [24] and FDIT, respectively.

Method \ Dataset	Church	CelebA-HQ	Waterfall
Im2StyleGAN [1]	219.50	-	267.25
StyleGAN2 [1]	57.54	-	57.46
Swap AE [24]	52.34	43.47	50.90
FDIT	48.21	42.02	48.76

Table 1: Results of FID on three datasets, *i.e.*, LSUN Church, CelebA-HQ, Mountains. Swap AE is short for Swapping Autoencoder [24]. FID of Im2StyleGAN, StyleGAN2 and Swap AE on Church and Waterfall datasets are reported from results in Swapping Autoencoder [24]

preserving the image content. Here we use Fréchet Inception Distance (FID) [11] as the measure of generated images’ quality. Results in Tab. 1 demonstrate that FDIT can impressively achieve lower FID across all datasets.

4.1.2 Image Attributes Editing

Our model is effective in not only the reference guided image generation task, but also the image editing task. The



Figure 5: Results on the CelebA-HQ [18] dataset. FDIT can generate more identity-preserving images than Swap AE [24]. In addition, compared to the state-of-the-art photorealistic style transfer method WCT2 [31], FDIT can synthesize cross-domain and photorealistic images.

identity-preserving results under the vector arithmetic operations and Principal Component Analysis (PCA) again demonstrate the universality and superiority of our proposed method.

Continuous interpolation between different domains.

Continuous interpolation aims at creating a series of smoothly changing images between two sets of distinct images. Vector arithmetic is one commonly used way to achieve this. For example, we can sample n images from each of the two target domains, and then compute the average difference of the vectors between these two sets of images:

$$\hat{\mathbf{z}} = \frac{1}{n} \sum_{i=0}^n \mathbf{z}_i^{\mathbf{d1}} - \frac{1}{n} \sum_{j=0}^n \mathbf{z}_j^{\mathbf{d2}}, \quad (11)$$

where $\mathbf{z}^{\mathbf{d1}}$, $\mathbf{z}^{\mathbf{d2}}$ denote the latent code from two domains, respectively.

This mean difference vector $\hat{\mathbf{z}}$ can be viewed as the directional vector from one domain to the other. Similar to the idea in InterFaceGAN [27], we can assume that there is a hyperplane lying between the latent codes of two domains. Therefore, a model will be better at the content-style disentanglement when the vector arithmetic results over one domain does not affect the representation of the other information.

In the experiment, we employ this method on the style code while keeping the content code unchanged. The generated images after continuous interpolation can be formalized as $\mathbf{x}_{\text{gen}} = G(\mathbf{z}_s, \mathbf{z}_t + \theta \cdot \hat{\mathbf{z}}_t)$, where θ denotes the



Figure 6: Image attributes editing results of the LSUN mountain dataset [33]. The central column denotes the source summer images, while within the remaining columns denote the continuous interpolation images targeting at autumn and winter.

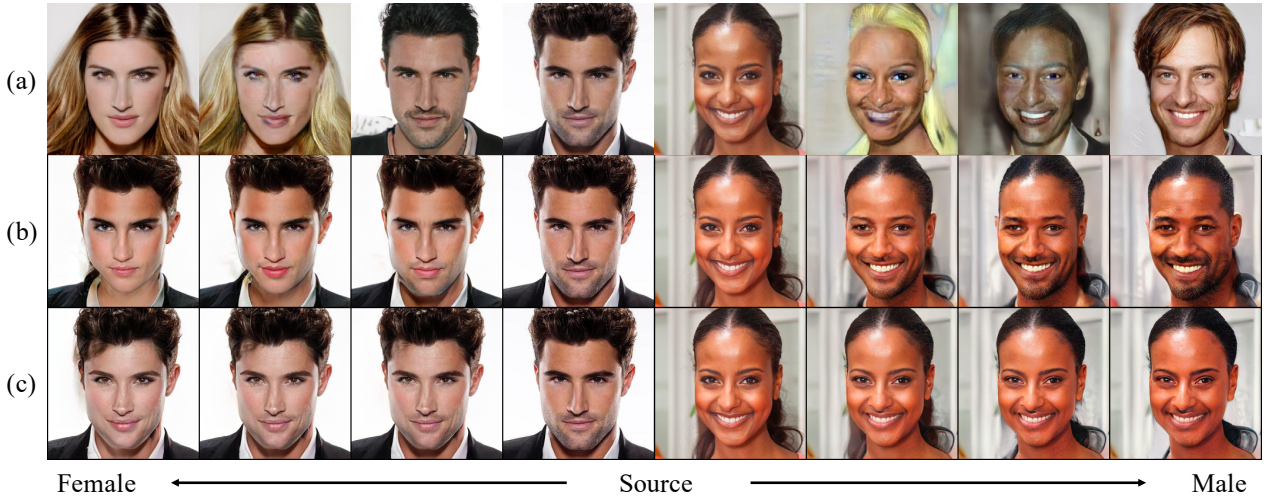


Figure 7: Image attributes editing results of the CelebA-HQ dataset. The central column denotes the source images, while within the remaining columns denote the continuous interpolation images targeting at male and female. (a) The semantic latent vectors in StarGAN v2 [6] are not continuous; (b) The vanilla Swapping AE [24] is in lack of identity-preserving capability; (c) The results of FDIT.

strength of that dragging directional vector. Results in Fig. 6 and Fig. 7 show that the directional vector \hat{z} extracted in our model can better achieve the image editing task along the target domain while strictly adhering to the content of the source image. Compared to the vanilla Swapping Autoen-

coder and StarGAN v2, our results demonstrate the better disentanglement ability of the proposed framework FDIT.

We also succeed to find disentangled semantic latent vectors via an unsupervised method, *i.e.*, Principal Component Analysis (PCA). The implementation details and the



Figure 8: GAN inversion results. For the given the (a) high-resolution source images, compared to (b) Image2StyleGAN[1], FDIT (c) achieves much better quality.

identity-preserving results are shown in Appendix 7.2.

4.2. GAN Inversion

State-of-the art GAN models StyleGAN [19] and StyleGAN2 [20] achieved epoch-making results in image generation, yet they are all noises-guided methods, meaning that they cannot tackle real-world images. Many approaches haven been [1, 2, 20] proposed to map the real images into those noise vectors.

Among them, Image2StyleGAN[1] is the pioneer work and achieves reasonable inversion performance. This approach can be viewed as a reconstruction model between the real image and the generated images via iterative optimization over the latent vector. Therefore, we impose the frequency based reconstruction loss on this model to further test our effectiveness on this brand-new task.

As shown in Fig. 8, after applying our method on the images with 1024×1024 resolution, the quality of the inverted images across all scenes is improved, especially the overall structure, fine details and color distribution.

4.3. StarGAN v2

StarGAN v2 is another state-of-the-art image translation model which could generate image hybrids guided by either reference images or latent noises. Here the style code \mathbf{z}_s is extracted by the style encoder. However, the content code is not explicitly extracted by a separate module. Instead, the source image is directly feed into the generator, where the style code \mathbf{z}_s is injected into it via AdaIN [12]. Similar to the autoencoder-based network, we can optimize the StarGAN v2 framework with our proposed model between the source, reference, and hybrid images. In order to validate FDIT in a stricter condition, we construct a CelebA-HQ-Smile dataset based on the smiling annotation in CelebA-HQ dataset. Here the style refers to whether that person smiles, and the content refers to the identity of that person,



Figure 9: StarGAN v2 results. Compared to vanilla StarGAN v2 [6], FDIT achieves much better identity-preserving ability.

such as the gender, personal face attributes, *etc.*

Results in Fig. 9 show that the advantages of adopting our model are three-fold. Firstly, FDIT can highly preserve the gender identity; in contrast, the vanilla StarGAN v2 model would change the resulting gender according to the reference image. Secondly, the image quality of FDIT is better, measured by FID. Thirdly, our model can change the smiling degree while maintaining other face attributes strictly.

5. Conclusion

In this paper, we have presented Frequency Domain Image Translation (FDIT) to improve the quality and the identity-preserving capability in image-to-image translation. On one hand, a *spatial level* restriction is introduced to locally preserve the frequency distribution. On the other hand, we have proposed a *spectral level* regulation to further enhance the distribution from a global perspective. Although being simple, the proposed approach have shown its effectiveness on a number of image translation datasets, and significantly improved the results of recent proposed Swapping Autoencoder [24], StarGAN v2 [6], and Image2StyleGAN [1]. Future research may focus on extending our method to other image generation tasks, such as super resolution, image inpainting and image composition.

6. Acknowledgment

Gao Huang is supported in part by the National Key R&D Program of China under Grant 2020AAA0105200, the National Natural Science Foundation of China under Grants 62022048 and 61906106, the Institute for Guo Qiang of Tsinghua University and Beijing Academy of Artificial Intelligence.

References

- [1] Rameen Abdal, Yipeng Qin, and Peter Wonka. Image2stylegan: How to embed images into the stylegan latent space? In *ICCV*, 2019. 2, 5, 6, 8, 12
- [2] R. Abdal, Y. Qin, and P. Wonka. Image2stylegan++: How to edit the embedded images? In *CVPR*, 2020. 2, 8
- [3] Andrew Brock, Jeff Donahue, and Karen Simonyan. Large scale gan training for high fidelity natural image synthesis. In *ICLR*, 2019. 2
- [4] Yunpeng Chen, Haoqi Fan, Bing Xu, Zhicheng Yan, Yan-nis Kalantidis, Marcus Rohrbach, Shuicheng Yan, and Jiashi Feng. Drop an octave: Reducing spatial redundancy in convolutional neural networks with octave convolution. In *ICCV*, 2019. 2
- [5] Yunjey Choi, Minje Choi, Munyoung Kim, Jung-Woo Ha, Sunghun Kim, and Jaegul Choo. Stargan: Unified generative adversarial networks for multi-domain image-to-image translation. In *CVPR*, 2018. 1, 2
- [6] Yunjey Choi, Youngjung Uh, Jaejun Yoo, and Jung-Woo Ha. Stargan v2: Diverse image synthesis for multiple domains. In *CVPR*, 2020. 1, 2, 5, 7, 8, 12
- [7] Jeff Donahue and Karen Simonyan. Large scale adversarial representation learning. In *NeurIPS*, 2019. 2
- [8] Ricard Durall, Margret Keuper, and Janis Keuper. Watch your up-convolution: Cnn based generative deep neural networks are failing to reproduce spectral distributions. In *CVPR*, 2020. 2
- [9] Ian Goodfellow, Jean Pouget-Abadie, Mehdi Mirza, Bing Xu, David Warde-Farley, Sherjil Ozair, Aaron Courville, and Yoshua Bengio. Generative adversarial networks. In *NeurIPS*, 2014. 2
- [10] Kaiming He, Xiangyu Zhang, Shaoqing Ren, and Jian Sun. Deep residual learning for image recognition. In *CVPR*, 2016. 5
- [11] Martin Heusel, Hubert Ramsauer, Thomas Unterthiner, Bernhard Nessler, and Sepp Hochreiter. Gans trained by a two time-scale update rule converge to a local nash equilibrium. In *NeurIPS*, 2017. 6
- [12] Xun Huang and Serge Belongie. Arbitrary style transfer in real-time with adaptive instance normalization. In *ICCV*, 2017. 2, 8
- [13] Xun Huang, Yixuan Li, Omid Poursaeed, John Hopcroft, and Serge Belongie. Stacked generative adversarial networks. In *CVPR*, 2017. 2
- [14] Xun Huang, Ming-Yu Liu, Serge Belongie, and Jan Kautz. Multimodal unsupervised image-to-image translation. In *ECCV*, 2018. 1, 2, 5
- [15] Kim Hyunsu, Jhoo Ho Young, Park Eunhyeok, and Yoo Sungjoo. Tag2pix: Line art colorization using text tag with secant and changing loss. In *ICCV*, 2019. 2
- [16] P. Isola, J. Zhu, T. Zhou, and A. A. Efros. Image-to-image translation with conditional adversarial networks. In *CVPR*, 2017. 1
- [17] Phillip Isola, Jun-Yan Zhu, Tinghui Zhou, and Alexei A Efros. Image-to-image translation with conditional adversarial networks. In *CVPR*, 2017. 5
- [18] Tero Karras, Timo Aila, Samuli Laine, and Jaakko Lehtinen. Progressive growing of gans for improved quality, stability, and variation. *arXiv preprint arXiv:1710.10196*, 2017. 5, 6
- [19] Tero Karras, Samuli Laine, and Timo Aila. A style-based generator architecture for generative adversarial networks. In *CVPR*, 2019. 2, 8, 12
- [20] Tero Karras, Samuli Laine, Miika Aittala, Janne Hellsten, Jaakko Lehtinen, and Timo Aila. Analyzing and improving the image quality of StyleGAN. In *CVPR*, 2020. 2, 5, 8
- [21] Nicholas Kolkin, Jason Salavon, and Gregory Shakhnarovich. Style transfer by relaxed optimal transport and self-similarity. In *CVPR*, 2019. 5
- [22] Christian Ledig, Lucas Theis, Ferenc Huszár, Jose Caballero, Andrew Cunningham, Alejandro Acosta, Andrew Aitken, Alykhan Tejani, Johannes Totz, Zehan Wang, et al. Photo-realistic single image super-resolution using a generative adversarial network. In *CVPR*, 2017. 2
- [23] Mario Lucic, Michael Tschannen, Marvin Ritter, Xiaohua Zhai, Olivier Bachem, and Sylvain Gelly. High-fidelity image generation with fewer labels. In *ICML*, 2019. 2
- [24] Taesung Park, Jun-Yan Zhu, Oliver Wang, Jingwan Lu, Eli Shechtman, Alexei A. Efros, and Richard Zhang. Swapping autoencoder for deep image manipulation. *arXiv preprint arXiv:2007.00653*, 2020. 1, 2, 5, 6, 7, 8, 11, 12, 13
- [25] Alec Radford, Luke Metz, and Soumith Chintala. Un-supervised representation learning with deep convolutional generative adversarial networks. *arXiv preprint arXiv:1511.06434*, 2015. 2
- [26] Yujun Shen, Jinjin Gu, Xiaoou Tang, and Bolei Zhou. Interpreting the latent space of gans for semantic face editing. In *CVPR*, 2020. 11
- [27] Yujun Shen, Ceyuan Yang, Xiaoou Tang, and Bolei Zhou. Interfacegan: Interpreting the disentangled face representation learned by gans. *arXiv preprint arXiv:2005.09635*, 2020. 6
- [28] Haohan Wang, Xindi Wu, Zeyi Huang, and Eric P Xing. High-frequency component helps explain the generalization of convolutional neural networks. In *CVPR*, 2020. 2
- [29] Xintao Wang, Ke Yu, Shixiang Wu, Jinjin Gu, Yihao Liu, Chao Dong, Yu Qiao, and Chen Change Loy. Esrgan: Enhanced super-resolution generative adversarial networks. In *ECCV*, 2018. 2
- [30] Kai Xu, Minghai Qin, Fei Sun, Yuhao Wang, Yen-Kuang Chen, and Fengbo Ren. Learning in the frequency domain. In *CVPR*, 2020. 2
- [31] Jaejun Yoo, Youngjung Uh, Sanghyuk Chun, Byeongkyu Kang, and Jung-Woo Ha. Photorealistic style transfer via wavelet transforms. In *ICCV*, 2019. 5, 6

- [32] Seungjoo Yoo, Hyojin Bahng, Sunghyo Chung, Junsoo Lee, Jaehyuk Chang, and Jaegul Choo. Coloring with limited data: Few-shot colorization via memory augmented networks. In *CVPR*, 2019. 2
- [33] Fisher Yu, Ari Seff, Yinda Zhang, Shuran Song, Thomas Funkhouser, and Jianxiong Xiao. Lsun: Construction of a large-scale image dataset using deep learning with humans in the loop. *arXiv preprint arXiv:1506.03365*, 2015. 5, 7, 11, 12
- [34] Jun-Yan Zhu, Taesung Park, Phillip Isola, and Alexei A Efros. Unpaired image-to-image translation using cycle-consistent adversarial networks. In *ICCV*, 2017. 1

7. Appendix

7.1. Visualization of the Adaptive Frequency Feature Embedding Module

In this paper, we propose to use the attention maps to help the image translation models learn the disentangled representation of the content and style information better. To demonstrate the effectiveness of our proposed Adaptive Frequency Feature Embedding (AFFE) module, we visualize the spectral response of such two kinds of the information under the FDIT assisted Swapping Autoencoder [24] model.

To be specific, we choose a layer after the AFFE module, and compute the FFT response of the features maps in the both content and style branch. Fig. 10 shows the average FFT distribution under the validation set of the LSUN Church [33] dataset. We can see that the FFT response of the content branch includes much more high frequency information than the style branch, while the style branch itself mainly contains the low frequency information. These results correspond to our observation in content-style decomposition in frequency domain, which in turn demonstrates the effectiveness of the AFFE module.

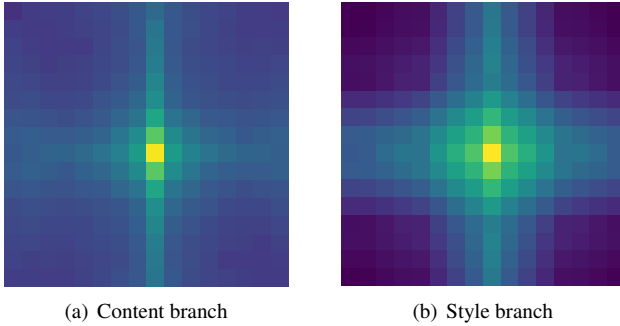


Figure 10: Visualization of the FFT response of a layer after the AFFE module in FDIT assisted Swapping Autoencoder [24] model. The brighter a point is, the greater the energy it has.

7.2. Unsupervised Semantic Vector Discovery for Image Editing

Besides continuous interpolation between different domains, another way of conducting vector arithmetic for image editing is to discover the underlying semantics \hat{z} via an unsupervised way. Here we adopt the Principal Component Analysis (PCA) [26] to achieve this goal, which could find the orthonormal components in the latent space. Similar to the continuous interpolation approach in our paper, when manipulating the style code using PCA, a good image translation model would keep the content of the images as untouched as possible.

Shown in Fig. 14, FDIT is once again demonstrated to be a better identity-preserving model. Specifically, the facial attributes are well maintained, while the only style information such as illumination and the hair color is changed.

7.3. Additional Frequency Domain Image Translation Results

Here we provide additional results of the autoencoder based FDIT model on Flickr Mountains, Flickr Waterfalls, and LSUN Bedroom [33] dataset.

Shown in Fig. 11, Fig. 12, and Fig. 13, our FDIT assisted Swapping Autoencoder [24] model achieves better performance in terms of the shape preserving, such as the outline of the mountains, the layout of the bedrooms, and the scene of the waterfalls.

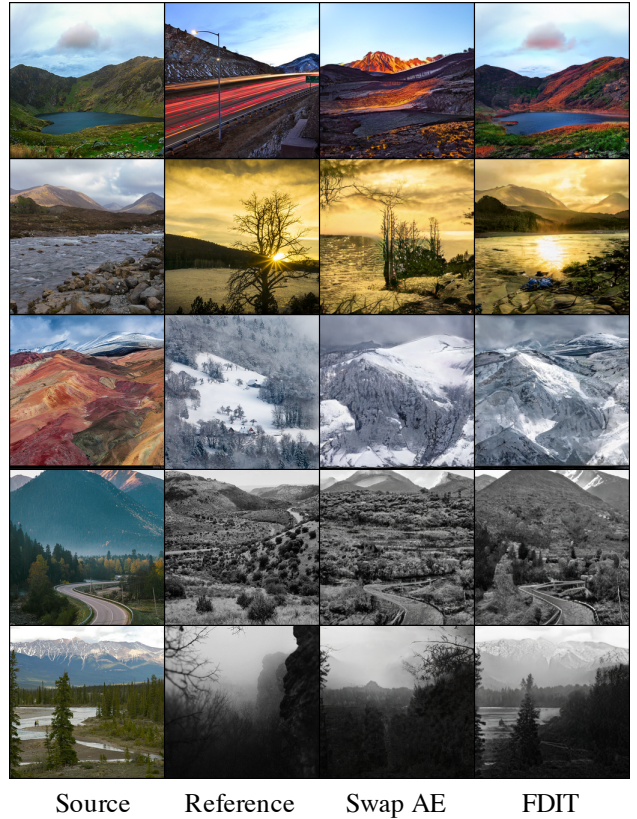


Figure 11: Image translation results of the Flickr Mountains dataset. Four columns denote the source images, reference images, and the generated images of Swapping Autoencoder [24] and FDIT, respectively.

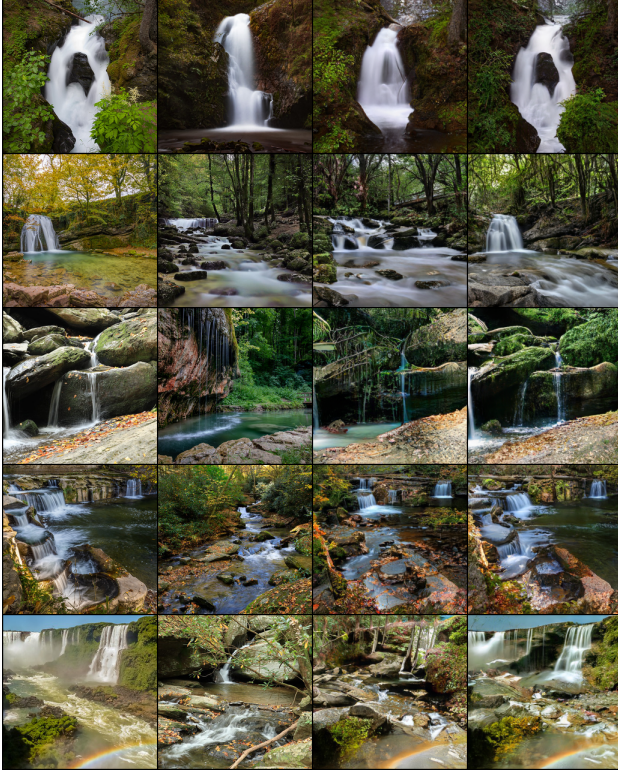


Figure 12: Image translation results of the Flickr Waterfalls dataset.

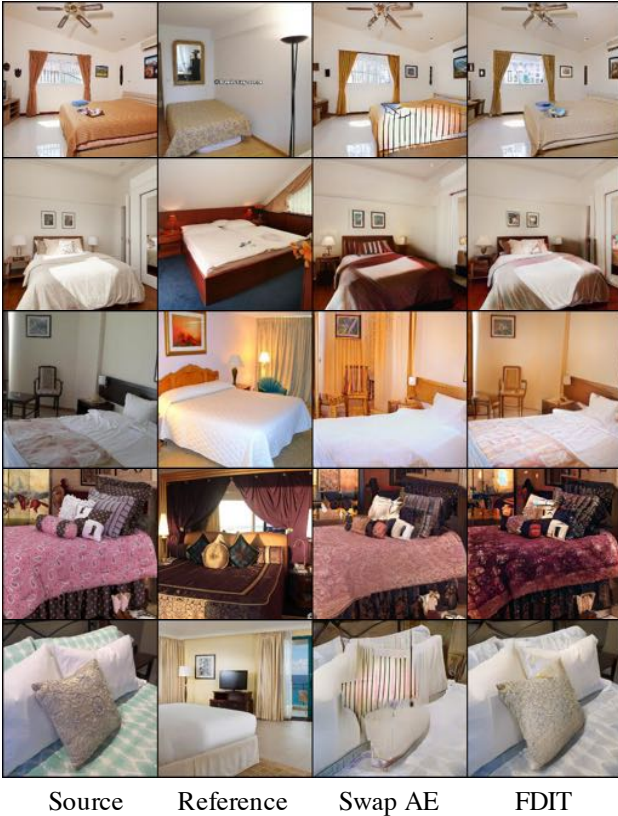


Figure 13: Image translation results of the LSUN Bedroom [33] dataset.

7.4. Additional Results on Flickr Faces HQ dataset

Flickr Faces HQ (FFHQ) dataset [19] is a large scale human face dataset which is composed of 70,000 high resolution aligned face images, collected from [flickr.com](https://www.flickr.com/). We randomly collect 200 images as the testing dataset. As shown in Tab. 2, our FDIT assisted model also surpasses the vanilla Swapping Autoencoder [24] in terms of the photo-realism.

Method \ Dataset	FFHQ
Im2StyleGAN [1]	123.13
StyleGAN2 [1]	81.44
Swap AE [24]	59.83
FDIT	55.96

Table 2: Results of FID on FFHQ dataset. Swap AE is short for Swapping Autoencoder [24]. FID of Im2StyleGAN, StyleGAN2 and Swap AE are reported from results in Swapping Autoencoder [24]

7.5. Additional StarGAN v2 Results

After incorporating the frequency based training objectives and the frequency domain assisted modules, our FDIT assisted StarGAN v2 [6] model can produce more photo-realistic image hybrids. Specifically, compared with the vanilla StarGAN v2 model, FID is improved from 17.32 to 16.86.



Figure 14: PCA based image attributes editing results of the FDIT assisted Swapping Autoencoder [24] model under the CelebA-HQ dataset. The central column denotes the source images, while within the remaining columns denote the continuous interpolation results of the orthonormal components along two directions.